Visible photoluminescence from silicon-ion-implanted SiO_2 film and its multiple mechanisms

H. Z. Song and X. M. Bao
National Laboratory of Solid State Microstructures and Department of Physics, Nanjing University, Nanjing 210093, People's Republic of China
(Received 1 October 1996)

Strong photoluminescence from silicon-ion-implanted thermal SiO_2 film was investigated under various conditions. The photoluminescence spectrum of as-implanted samples or samples annealed in N_2 at a temperature below 1000 °C consists of three bands centered at about 470, 550, and 630 nm. Annealing at a temperature above 1000 °C for a long enough time brings about one photoluminescence band peaking at about 730 nm. The peak wavelengths of these four bands are all independent of annealing or excitation conditions. As the annealing temperature is increased, 470-, 550-, and 630-nm bands are initially intensified and then weakened with the intensity maxima at 600, 300, and 200 °C, respectively; as the annealing time increases from 1 min, they are monotonously weakened. The 730-nm band is always strengthened whether with increasing annealing time or temperature within our experimental range. In addition, these four bands show different excitation behaviors. The discussion section argues that the 470-, 550-, and 630-nm bands result from different point defects in the bulk of silicon implanted SiO_2, while the 730-nm one results from luminescence centers at the interface between the nanocrystal silicon and SiO_2 matrix. [S0163-1829(97)03011-7]

I. INTRODUCTION

The observation of intense visible luminescence at room temperature from low-dimensional silicon structures[1] created an opportunity for incorporating optoelectronic functions in silicon integrated-circuits technology. From then on, countless studies focused on silicon-based light-emitting materials. Following the electrochemical technique fabricating porous silicon,[1] many other methods such as plasma deposition from silane,[2–5] silicon-ion implantation into SiO_2,[6–11] glass-melt reaction,[12] crystallization of amorphous silicon,[13] silicon and SiO_2 rf cosputtering,[14] and reactive ion-etching techniques[15] were used to make silicon nanostructures. Among these, the most attention was paid to silicon-ion-implanted SiO_2 because of many advantages of the method of ion implantation: routinely used in integrated-circuits technology, enhancing the mechanical and thermal stability, and enabling one to rule out some of the alternative luminescence sources. Shimizu-Iwayama *et al.*[6] used silicon-implanted silica glass to prepare silicon nanostructure and obtained visible photoluminescence (PL). They observed two bands at 1.9 and 1.7 eV, and ascribed them to E' center defects and the presence of silicon nanocrystals, respectively.[6–9] Thermally grown SiO_2 is much closer to silicon-based light-emitting materials, and much more compatible to the microelectronic technology than silica glass, so silicon-implanted thermal SiO_2 grown on crystal silicon is a promising candidate for silicon-based light-emitting materials. With respect to this system, Komoda *et al.*[11] reported 600–800-nm luminescence, and Mutti *et al.*[10] observed 490–540-nm luminescence. They both ascribed the luminescence to quantum confinement of nanocrystal silicon. Cheong *et al.*[6] supplied more evidence for the quantum confinement effect by the hydrostatic pressure measurement. However, Liao *et al.*[17,18] observed 470- and 550- nm emission and found them defect related. It seems that there are multiple luminescence origins for silicon-implanted SiO_2. Considering the controversial luminescence mechanism and a lack of overall knowledge, we intend to study the PL evolution of the silicon-implanted thermal SiO_2 layer in a wide treatment and measurement range, to show a complete description of the luminescence property of this prospective silicon-based light-emitting material.

II. EXPERIMENTS AND RESULTS

Samples were prepared by Si^+ implantation at an energy 120 keV and with a dose 2×10^{16} cm^{-2}, at room temperature, into the SiO_2 layer thermally grown on (100)-oriented, 5 Ω cm, p-type silicon substrate. The thickness of the SiO_2 layer was 360 nm. The implantation region is at a depth between 90 and 170 nm below the surface. Silicon-implanted wafers were subsequently annealed at temperatures from 100 °C to 1150 °C in a controlled N_2 atmosphere. Annealing for shorter than 2 min was performed in a KST-2 rapid thermal processor, and that for a longer time was in a quartz furnace. The PL spectra and PL excitation (PLE) spectra were measured on a Hitachi 850 fluorescence spectrophotometer at room temperature. The excitation wavelength is 250 nm in this work unless noted otherwise.

Intense visible light emission from our samples was easily observed at room temperature. The samples with the strongest PL have intensities higher than 10% of that for a typical aged porous silicon sample under the same ultraviolet excitation. As shown in Fig. 1, the PL spectrum for the as-implanted sample without annealing or the sample annealed below 1000 °C (these two cases will be just termed as ''below 1000 °C'' in the following text) appears broad with a tail at the longer-wavelength side. Comparing the PL spectra of as-implanted and 600 °C, 60-min annealed samples in Fig. 1, it can be seen that the spectrum tails become relatively weaker with annealing. Through a number of spectrum decompositions, it is found that each of these PL spectra is composed of three bands located at about 470, 550, and 630

0163-1829/97/55(11)/6988(6)/$10.00 © 1997 The American Physical Society

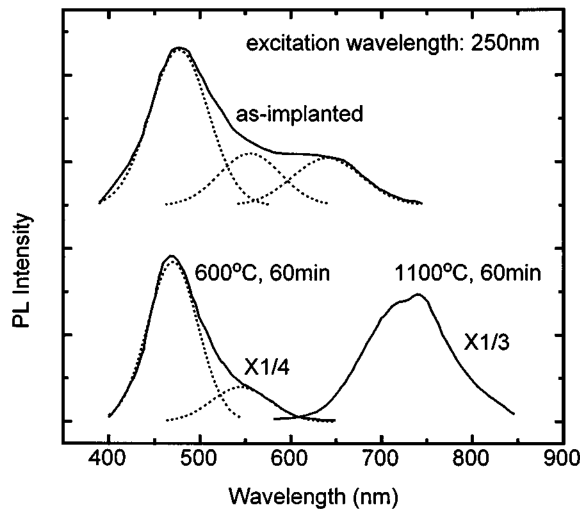

FIG. 1. Typical PL spectra for an as-implanted sample and samples annealed at 600 °C for 60 min and at 1100 °C for 60 min. The dashed lines show the decomposed PL bands at about 470, 550, and 630 nm.

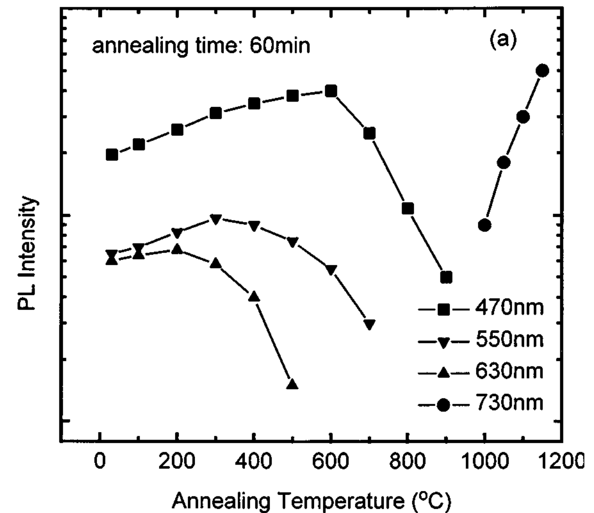

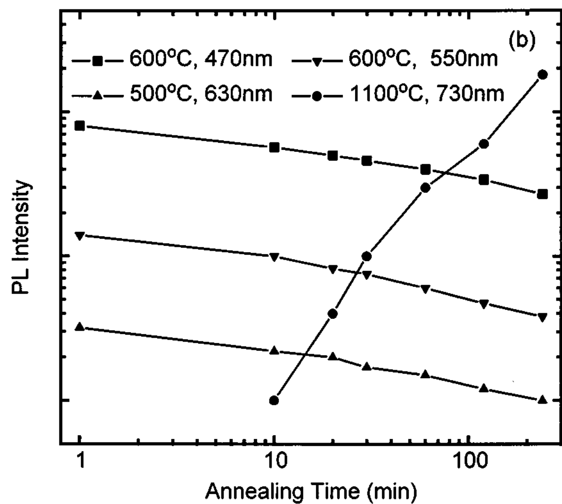

FIG. 2. Dependencies of the PL intensity on (a) annealing temperature and (b) annealing time for the four PL bands at 470, 550, 630, and 730 nm. A common annealing time of one hour is chosen for any band in (a), but different temperatures are selected in (b) for different bands. Note that the scales of intensity and time are logarithmic.

nm. Their peak positions change little with the annealing condition. Naturally, the shape evolution of the PL spectrum with annealing below 1000 °C is caused just by the relative variation between the three bands. As shown in Fig. 1, the intensity of the 550- or 630-nm band is about one-third of that for the 470 nm one in the PL spectrum of the as-implanted sample. A higher annealing temperature leads to weaker 550- and 630-nm bands compared with the 470 nm one, and the 630-nm band decreases more rapidly with annealing temperature than the 550 nm one. Figure 1 shows us an example: after annealing at 600 °C for 60 min, the intensity of the 550-nm band is reduced to one-forth of 470-nm band, and the 630-nm band disappears. When the annealing temperature is above 1000 °C, the above three bands are quenched; in the mean time, another PL spectrum appears if the annealing time is more than 10 min. As shown in Fig. 1, the PL spectrum for 1100 °C, 60 min annealing is centered at about 730 nm. However, annealing never changes the peak position and the shape of the spectrum obtained by annealing above 1000 °C, so it can be regarded as one band.

By now, we have observed four PL bands, two stronger at 470 and 730 nm and two weaker at 550 and 630 nm, from silicon-implanted thermal SiO_2. Now let us observe their variations in detail. At first, the full width at half maximum (FWHM) of all four PL bands weakly decrease with increasing annealing temperature and time (not shown). Figure 2 shows the temperature and time dependencies of the integrated intensity for each band. As can be seen in Fig. 2(a), the 470-, 550-, and 630-nm bands have a similar annealing behavior: with increasing temperature, the PL intensity first increases slowly and then decreases rapidly in an isochronal annealing. The maxima for 470-, 550-, and 630-nm bands are at 600, 300, and 200 °C, respectively. Obviously, the 470-nm band is the most stable among these three bands. However, the 730-nm band monotonously increases with increasing annealing temperature from 1000 °C to 1150 °C. Figure 2(b) shows that the 470-, 550-, and 630-nm bands decrease with annealing time at similar rates (at 600 or 500 °C), but the 730 nm band increases more rapidly with annealing time (at 1100 °C). As a matter of fact, this result is qualitatively true for any effective temperature. Additionally, although the 730-nm band cannot be detected for shorter annealing, it is very stable once produced.

The observed PL spectra also vary with the excitation wavelength. In Fig. 3, one can observe a redshift of the PL spectrum for 600 °C, 60-min annealed sample with the increasing excitation wavelength. Spectrum decompositions show that with increasing excitation wavelength, the 470-nm band decreases, while the 550 nm one increases and then becomes the sole band under 300-nm excitation. In general, longer-wavelength excitation brings about a relatively stronger emission of 550- and 630-nm bands compared with the 470 nm one. The 550- and 630-nm bands increase almost at the same rate. Finally, the PL spectra never shift when the excitation wavelength is longer than 300 nm. The PL band for annealing above 1000 °C, exhibits no change in shape and FWHM with excitation wavelength.

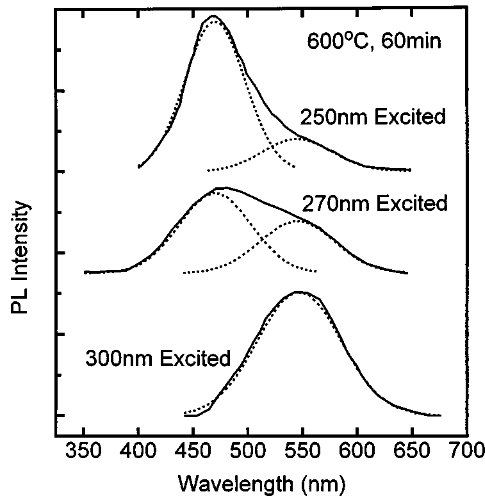

FIG. 3. Typical PL spectra for 600 °C, 60-min annealing under different excitation wavelengths and their decomposed bands at 470 and 550 nm which are shown by dashed curves.

To clarify the photoabsorption process of each PL band, we measured the PLE spectra at various emission positions, which are shown in Fig. 4. Although annealing can change the PLE intensity, it cannot change the PLE spectra shapes at 470, 550, and 630 nm. The PLE spectrum monitored at 470-nm emission is a sharp (FWHM 20-nm) peak around 250 nm. That at 550 nm includes the 250-nm peak together with a shoulder around 280–290 nm. The 630-nm emission has a PLE spectrum almost the same as that of 550 nm. However, the PLE spectrum of the 730-nm band is different from the other three. As shown in Fig. 4, it has a background absorption, which decreases with increasing wavelength. On this background is superimposed a sharp peak at 230 nm and another weak shoulder. More noticeably, a broad PLE peak appears at longer wavelengths, and it redshifts with increas-

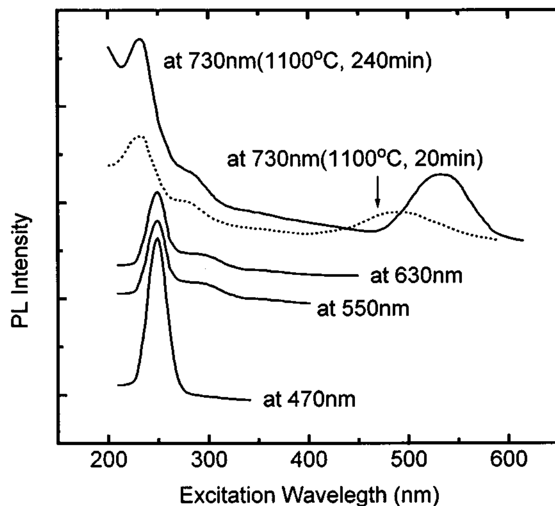

FIG. 4. PLE spectra monitored at 470, 550, and 630 nm for any treatment, and that at 730 nm for annealing at 1100 °C for different times. The intensity scales for 470-, 550-, and 630-nm emission are selected arbitrarily since their shapes are independent of annealing, but both spectra for 730 nm have the same intensity scale.

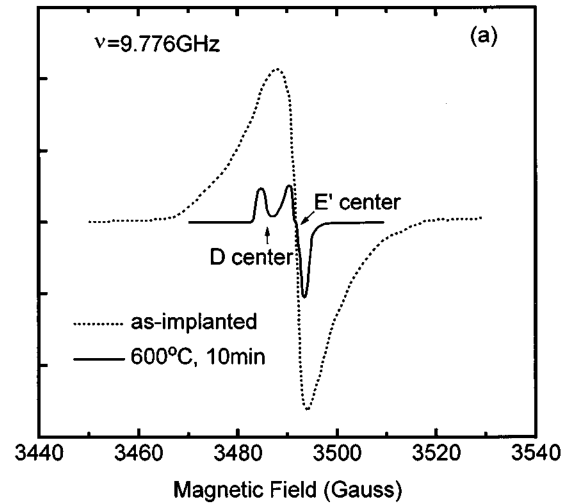

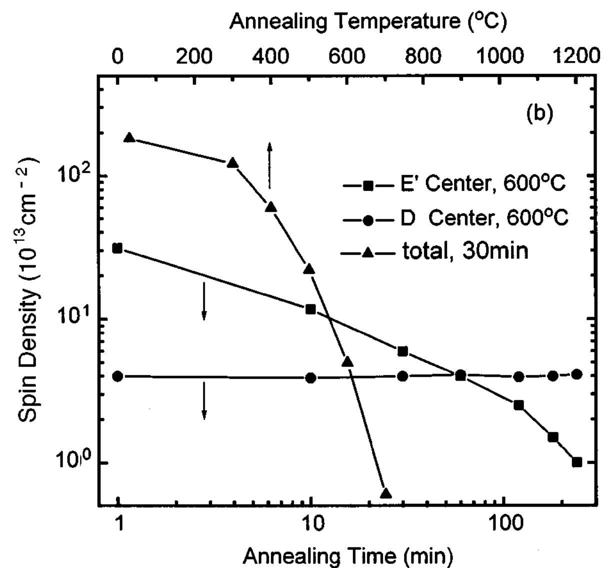

FIG. 5. (a) EPR spectra for as-implanted and 600 °C, 10-min annealed samples; (b) temperature dependence of the total spin density for one hour of annealing, and time dependences of the spin densities of E' centers and D centers for annealing at 600 °C. Note that the scales of spin density and time are logarithmic.

ing annealing temperature and time. In Fig. 4, we show the results of two samples annealed for 20 and 240 min at 1100 °C for comparison.

In order to reveal the microstructure evolution which may be responsible for the observed PL property, we measured the electron paramagnetic resonance (EPR) and x-ray photoelectronic spectra (XPS). From Fig. 5(a), the as-implanted sample was found to involve a broad resonance line for the E' center defect ($O_3{\equiv}Si\cdot\ \cdots{}^{+}Si{\equiv}O_3$ or $\cdot Si{\equiv}O_3$).[9,10,19,20] The large width for E' centers has been ascribed to homogeneous broadening by the dipole-dipole interaction.[21] The asymmetry of this EPR spectrum suggests that it includes other lines besides the E' center. Longer annealing time, especially higher annealing temperature results in the sharper and weaker EPR spectrum and then makes the spectrum structure more and more clear. A typical EPR spectrum for 600 °C, 10-min annealing is also shown in Fig. 5(a), from which we can see the sharpened E' line together with an-

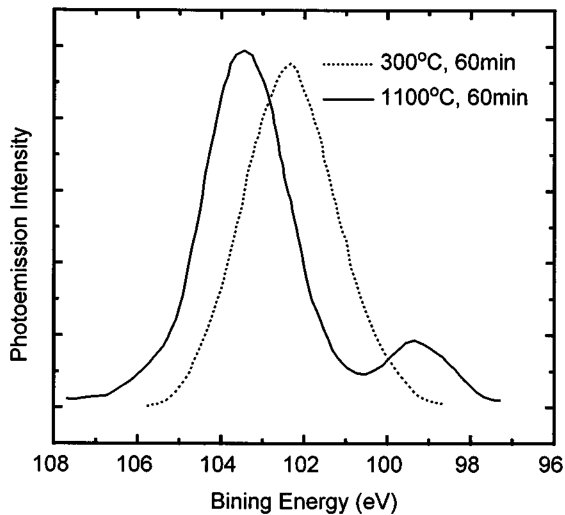

FIG. 6. Two typical XPS spectra for a Si $2p$ core level after annealing at 300 °C for 60 min and at 1100 °C for 60 min.

other low-field resonance, which has been referred to as the D center $((\cdot Si\equiv Si_3)_n)$.[9] In fact, due to their large width, the E' and D center cannot be resolved separately until 400 °C annealing. We estimated the spin density by comparing the resonance area with that of a known standard sample. The total spin density versus temperature is shown in Fig. 5(b). Different from the temperature dependence of the PL intensity in Fig. 2(a), the spin density just degrades with temperature, which is not in accordance with the reports by Shimizu-Iwayama *et al.*[9] who observed a correlation between E' defects and a PL intensity for silicon-implanted silica glass. At temperatures higher than 800 °C, the spin density is below the detection limit of our EPR instrument. In Fig. 5(b), also shown are spin-density variations of E' and D centers at 600 °C with annealing time. It is clear that D centers keep almost constant, but E' centers remarkably decrease with increasing time. Another fact that E' centers degrade more rapidly than the PL intensity in isothermal annealing supplies us with more evidence for no exact correlation between the E' center and PL in our samples. In fact, D centers also decrease with increasing temperature, but much slower than the E' center. XPS was measured focusing on the implantation layer. It is found that the samples as-implanted and annealed below 1000 °C show their broadened XPS peak of silicon $2p$ core level at positions lower than 103.4 eV, which is that of stoichiometric SiO_2. Figure 6 shows us a XPS peak at 102.3 eV corresponding to 300 °C, 60-min annealing. This kind of lower energy XPS has been reported for silicon-riched oxide, SiO_x (see Ref. 29, Cooke *et al.*). We noted that the XPS peak deviation from standard SiO_2 coexists with the PL for annealing below 1000 °C. With increasing annealing temperature and time, this peak sharpens and gradually shifts towards 103.4 eV. When the annealing temperature is at 1000 °C or higher, this peak is located at 103.4 eV and never shifts, while a different peak at about 99.4 eV appears, as shown in Fig. 6. This peak corresponds to that for crystal silicon, and becomes more and more intense with increasing temperature and time. The above facts imply that, with a strengthened annealing condition, the as-implanted homogeneous SiO_x network tends to be separated into the following two phases: SiO_2 and crystal silicon. More important, this evolution correlates with the appearance of the 730-nm PL band.

III. DISCUSSION

The original purpose of silicon implantation into SiO_2 is to form silicon nanostructure buried in oxide matrix, and to realize strong visible-light emission from quantum confinement of nanocrystal silicon. The detected D centers in our samples supply evidence for the existence of silicon clusters scattered in the silicon-implanted thermal SiO_2 layer. For D centers, the slower decrease with temperature and little variation with time mean their better stability, especially the precipitation trend of silicon atoms under thermal treatment. However, the silicon cluster will not be well crystallized until a critical temperature. The appearance of 99.4-eV XPS peak for crystal silicon only above 1000 °C implies that crystallized silicon particles, nanosized from many reports,[7–9] will not be numerously produced until annealing above 1000 °C, which is in accordance with the reported results of transmission electronic microscopy.[7]

According to the above discussion about microstructure, the PL of samples annealed below 1000 °C may not be ascribed to nanocrystal silicon, but to the bulk silicon oxide. As is well known, the visible luminescence centers in SiO_2 are various defects. Almost all intrinsic point defects of SiO_2 can be formed by ion implantation. Therefore, the three PL bands for samples treated below 1000 °C should be interpreted by the defects in the silicon-implanted layer in SiO_2. The 470-nm (2.7-eV) PL has been thoroughly studied in silica glass[22,23] and ion-implanted SiO_2 layer.[24] Hayes *et al.*[23] associated this emission with a transient pair of oxygen vacancy and oxygen interstitial. This is less reasonable for our samples because all of them are oxygen deficient. The 250-nm (5 eV) PLE peak of the 470-nm PL band is often observed in SiO_2 and has been proved corresponding to the photoabsorption of neutral oxygen vacancy defect $(O_3\equiv Si-Si\equiv O_3)$.[22] Consequently, the 470-nm PL band is caused by neutral oxygen vacancy, which agrees with the conclusion by Tohmon *et al.*[22] and Nishikawa *et al.*[24] Although the PLE of 550- and 630-nm band includes the 250-nm peak, their difference from that of 470-nm band is apparent. They should be associated with other defects. As we know, any bulk point defect in SiO_2 has not been observed to be related to a PL band around 550 nm. With silicon implantation in a large quantity into SiO_2, Mutti *et al.*[10] observed stable PL at 540 nm after 1000 °C annealing, and they think it resulted from quantum confinement effect. Nonetheless, this band is often observed without thermal treatment at high temperature. The 550-nm band must be assigned as due to some defect in SiO_2, with the microstructure presently unsettled. As referred to the 630-nm PL band, Shimizu-Iwayama *et al.*[9] ascribed it to the E' defect according to their observed identical dependencies on temperature for their silica samples. In our results there is not such an exact correlation, so we do not think of the E' center defect as the just origin of 630-nm PL for silicon-implanted thermal SiO_2. In SiO_2, another radiative defect is the nonbridging oxygen hole center (NBOHC), whose luminescence resembles our observed 630-nm PL band.[25,26] As a local oxy-

gen excess center, the NBOHC must be unstable and very low in density in our oxygen-deficient material. As a result, the 630-nm PL is the weakest and the most unstable among the three bands for annealing below 1000 °C. It is plausible for us to regard the NBOHC as the very origin of the 630-nm luminescence band.

What is the role of the E' center defect, which is the main EPR signal in the implantation layer? It is necessary to take account of the nonradiative recombination (NRR) effect in our samples. Since the E' center is a hole trap and defect degrading the electronic properties of thin-film SiO_2,[24] we may regard it as a NRR center. Then, its decrease brings about an increase in PL intensity.[17] Nevertheless, the radiative center such as the neutral oxygen vacancy, as a defect produced by implantation, also decreases with increasing annealing time and temperature. That is the very reason for the observed PL degradation by isothermal annealing. From the chemical stability, it may be certain that the bonded neutral oxygen vacancy is more stable than the E' center with a dangling bond. Provided that the radiative centers are reduced more slowly than the NRR centers, the temperature dependencies of PL intensity for the three bands at 470, 550, and 630 nm can be easily explained. With increasing temperature, the decrease of the NRR probability first predominates in PL variation, so all the three bands become stronger and stronger. When the NRR centers are greatly quenched, the decrease of radiative centers will be more prevalent, which inevitably weakens the PL.

The distinct behavior of the 730-nm PL band from the other three suggests its special luminescence mechanism. Experiments indicate that the appearance of 730-nm band is correlated with the crystallization of nanosized silicon and the disappearance of defects. It is certain that the mean size of nanocrystal silicon particles, will increase with annealing time at a high temperature.[7] However, the little dependence of the peak position of the 730-nm band on the annealing condition conflicts with an explanation by quantum confinement of nanocrystal silicon. Thus, it can only originate from the interface between nanocrystal silicon and disordered SiO_2.[7–9] In detail, it is some localized luminescence center at the interface that is responsible for 730-nm emission. Stronger treatment means a larger interface area, including nanocrystal silicon increase in size and number. As a result, the 730-nm PL intensity rises with increasing annealing temperature and time. In the PLE spectrum, the characteristic absorption band at 230 nm cannot be ascribed to point defect because of the diminished defect density. It is most probably also from the interface between nanocrystal silicon and SiO_2. More important, the shifting PLE band in the longer wavelength range can be reasonably referred to as the optical-absorption transition inside nanocrystal silicon. Its redshift results from the decreased band gap. The absorption inside nanocrystal silicon together with the emission process at the interface has been described in the luminescence mechanism of porous silicon suggested by Koch *et al.*[27] and Qin and Jia[28] which have been supported by more and more experimental results.[29] After annealed at temperatures higher than 1000 °C, silicon-implanted SiO_2 film is much like porous silicon in structure, i.e., nanocrystal silicon surrounded by an amorphous matrix, so it is comprehensive for them to have the same photoluminescence mechanism. On the other hand, the interfacial luminescence center emitting 730-nm light has never been found for the interface between bulk silicon and the SiO_2 layer, but often observed in oxidized porous silicon.[29] It may be a certain local state which is produced only at the interface between nanocrystal silicon and amorphous silicon oxide.

The PL so far observed from silicon-implanted thermal SiO_2 has covered the whole visible range. This is helpful and valuable to application research. Due to the lack of an intensity balance between different luminescence bands, however, it is urgent to thoroughly improve the luminescence efficiency. The photoabsorption of nanocrystal silicon provides an available path to strengthen the PL. That is to construct nanocrystal silicon particles small enough together with the numerous presence of the luminescence centers. Another topic for further study is to separate those coexisting defects produced by ion implantation to obtain single band emission.

In summary, we systematically investigated the PL of silicon-implanted thermal SiO_2 film. The PL of samples annealed below 1000 °C (including as-implanted) and above 1000 °C were discovered to have different behaviors. The former is composed of three PL bands at 470, 550, and 630 nm, which show an intensity maxima at 600, 300, and 200 °C, respectively, in isochronal annealing and decrease at similar rates with time in isothermal annealing. The latter, a band at 730 nm, always rises with increasing annealing temperature and time in our measurement range. Among these four PL bands, 470 and 730 nm are strong and stable, while 550 and 630 nm are weak and unstable. Microstructure analysis and excitation research indicate that the 470-, 550-, and 630-nm bands originate from different defects in the silicon-implanted SiO_2 layer, while the 730-nm band results from luminescence centers at the interface between nanocrystal silicon and silicon oxide matrix.

ACKNOWLEDGMENT

This work was supported by National Science Foundation of China and Ion Beam Laboratory, Shanghai Institute of Metallurgy, Chinese Academy of Science.

[1] For example, L. T. Canham, Appl. Phys. Lett. **57**, 1046 (1990).

[2] T. Kawaguchi and S. Miyamiza, Jpn. J. Appl. Phys. **32**, L215 (1993).

[3] D. Zhang, R. M. Kolbas, P. D. Milewski, D. J. Lichtenwalner, A. I. Kingon, and J. M. Zavada, Appl. Phys. Lett. **65**, 2684 (1994).

[4] P. D. Milewski, D. J. Lichtenwalner, P. Mehta, A. I. Kingon, D. Zhang, and R. M. Kolbas, J. Electron. Mater. **23**, 57 (1994).

[5] S. Tong, X. N. Liu, and X. M. Bao, Appl. Phys. Lett. **66**, 469 (1995).

[6] T. Shimizu-Iwayama, M. Ohshima, T. Niimi, S. Nakao, K. Saitoh, T. Fujita, and N. Itoh, J. Phys. Condens. Matter **5**, L375 (1993).

[7] T. Shimizu-Iwayama, S. Nakao, K. Saitoh, and N. Itoh, J. Phys.

Condens. Matter **6**, L601 (1994).
[8] T. Shimizu-Iwayama, S. Nakao, and K. Saitoh, Appl. Phys. Lett. **65**, 1814 (1994).
[9] T. Shimizu-Iwayama, K. Fujita, S. Nakao, K. Saitoh, T. Fujita, and N. Itoh, J. Appl. Phys. **75**, 7779 (1994).
[10] P. Mutti, G. Ghisloti, S. Bertoni, L. Bonoldi, G. F. Cerofolni, L. Meda, E. Grilli, and M. Guzzi, Appl. Phys. Lett. **66**, 851 (1995).
[11] T. Komoda, J. Kelly, F. Cristiano, A. Nejim, P. L. F. Hemment, K. P. Homewood, R. Gwilliam, J. E. Mynard, and B. J. Sealy, Nucl. Instrum. Methods Phys. Res. Sect. B **96**, 387 (1995).
[12] S. H. Risbud, L.-C. Liu, and J. F. Shackelford, Appl. Phys. Lett. **63**, 1648 (1993).
[13] X. Zhao, O. Schoenfeld, J. Kusano, Y. Aoyagi, and T. Sugano, Jpn. J. Appl. Phys. **33**, L649 (1994).
[14] Q. Zhang, S. C. Bayliss, and R. A. Hutt, Appl. Phys. Lett. **66**, 1977 (1995).
[15] A. G. Nassiopoulos, S. Grigoropoulos, E. Gogolides, and D. Papadimitriou, Appl. Phys. Lett. **66**, 1114 (1995).
[16] H. M. Cheong, W. Paul, S. P. Withrow, J. G. Zhu, J. D. Budai, C. W. White, and D. M. Hembree, Appl. Phys. Lett. **68**, 87 (1996).
[17] L. S. Liao, X. M. Bao, X. Q. Zheng, N. S. Li, and N. B. Min, Appl. Phys. Lett. **68**, 850 (1996).
[18] L. S. Liao, X. M. Bao, N. S. Li, X. Q. Zheng, and N. B. Min, J. Lumin. **68**, 199 (1996).
[19] H. Hosono, J. Appl. Phys. **69**, 8079 (1991).
[20] E. H. Poindexter and P. J. Caplan, J. Vac. Sci. Technol. A **6**, 1352 (1988).
[21] T. Fujita, M. Fukui, S. Okada, T. Shimizu, and N. Itoh, Jpn. J. Appl. Phys. **28**, L1254 (1989).
[22] R. Tohmon, Y. Shimogaichi, H. Mizuno, Y. Ohki, K. Nagasawa, and Y. Hama, Phys. Rev. Lett. **62**, 1388 (1989).
[23] W. Hayes, M. J. Kane, O. Salminen, R. L. Wood, and S. P. Doherty, J. Phys. C **17**, 2943 (1984).
[24] H. Nishikawa, E. Watanabe, D. Ito, M. Takiyama, A. Leki, and Y. Ohki, J. Appl. Phys. **78**, 842 (1995).
[25] L. Skuja, Solid State Commun. **84**, 613 (1992).
[26] L. N. Skuja, A. N. Streletskey, and A. B. Pakovich, Solid State Commun. **50**, 1069 (1984).
[27] F. Koch, V. Petrova-Koch, T. Maschik, A. Nikolov, and V. Gavrilenko, in *Microcrystalline Semiconductors: Materials Science & Devices*, edited by P. M. Fauchet, C. C. Tsai, L. T. Canham, I. Shimizu, and Y. Aoyagi, MRS Symposia Proceedings No. 283 (Materials Research Society, Pittsburgh, 1993), p. 197.
[28] G. G. Qin and Y. Q. Jia, Solid State Commun. **86**, 559 (1993).
[29] For example, L. Tsybeskov and P. M. Fauchet, Appl. Phys. Lett. **64**, 1983 (1994); G. G. Qin, H. Z. Song, B. R. Zhang, J. Lin, J. Q. Duan, and G. Q. Yao, Phys. Rev. B **54**, 2548 (1996); D. W. Cooke, B. L. Bennett, E. H. Farnum, W. L. Hults, K. E. Sickafus, J. F. Smith, J. L. Smith, T. N. Taylor, P. Tiwari, and A. M. Portis, Appl. Phys. Lett. **68**, 1663 (1996).